

**Supplementary information – Monte Carlo
simulations of complexation between weak
polyelectrolytes and a charged nanoparticle.
Influence of polyelectrolyte chain length and
concentration.**

Morten Stornes,[†] Per Linse,[‡] and Rita S. Dias^{*,†}

*[†]Department of Physics, NTNU - Norwegian University of Science and Technology,
NO-7491 Trondheim, Norway*

*[‡]Division of Physical Chemistry, Center for Chemistry and Chemical Engineering, Lund
University, S-22100 Lund, Sweden*

E-mail: rita.dias@ntnu.no

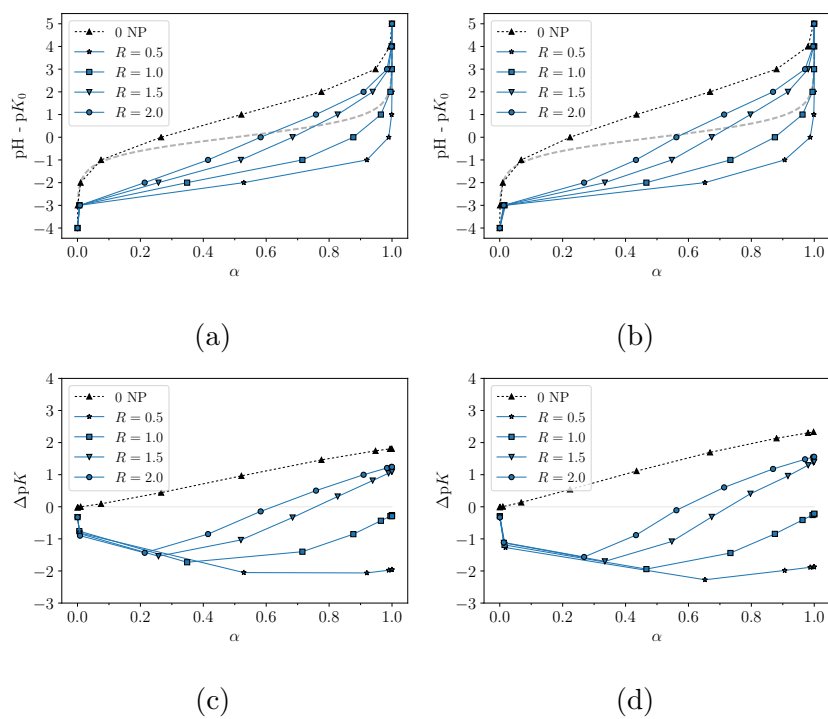


Figure S1: Titration curves and variation in ΔpK at different R for chain lengths $N_{mon} = 6$ (left) and $N_{mon} = 10$ (right)

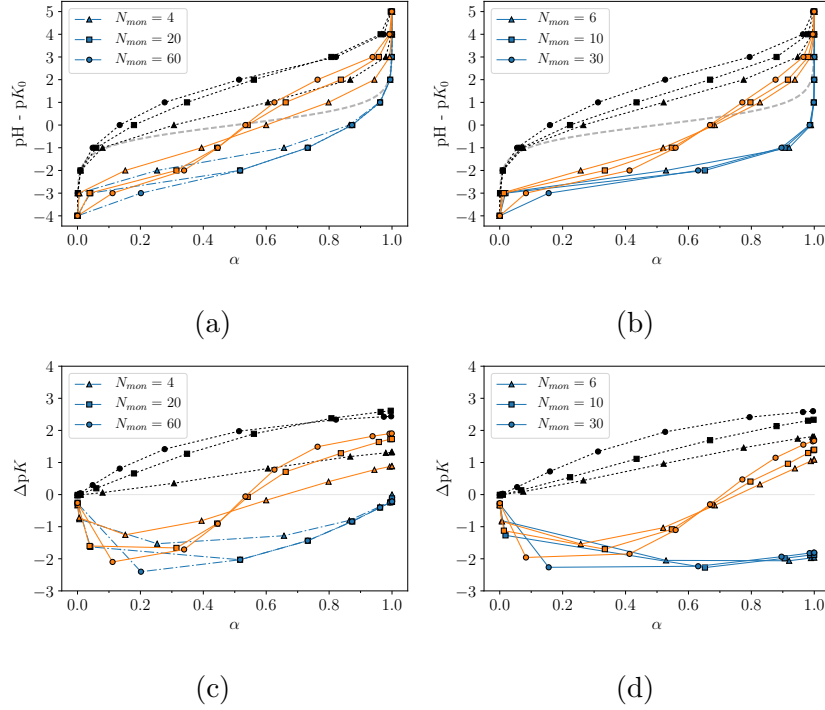


Figure S2: Titration curves showing the increase in ionization with pH (top) and the difference between the apparent and intrinsic dissociation constant for increasing ionization (bottom). Left side shows results for chain lengths not included in the main paper with $R = 1.0$ (dash-dotted blue lines) and $R = 2.0$ (solid orange lines), while right side refers to systems with chains of 6, 10, and 30 monomers and mixing ratios of $R = 0.5$ (blue lines) and $R = 1.5$ (solid orange lines). Only shown for integer values of $\text{pH} - \text{p}K_a$.

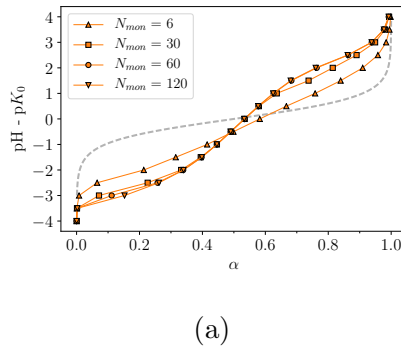


Figure S3: Titration curves for systems with longer chains at $R = 2$, showing the convergence of the titration curves as the chain length increases.

Figure S4 shows additional information regarding the systems discussed in relation to the charge profile of the adsorbed PA chains and Figure 4.

We start by defining $\overline{Z}_i = (Z_i + Z_{N_{mon}-i+1})/2$ for $i \in [1, N_{mon}/2]$, that is, \overline{Z}_i gives the average charge of monomers at equal distance from the ends of the chain. Taking into account the systems containing $N_{mon} = 30$, \overline{Z}_1 and Z_{mid} correspond to the average charge of the end and the middle monomers, respectively. Figure S4a and Figure S4b show the index, i , of maximum and minimum average charge, \overline{Z}_i , respectively.

It is interesting to see that the maximum charge is located either at the ends ($i = 1$) or very close to the center of the chain ($12 \leq i \leq 15$). The maximum charge is located close to the center of the chain for α^{ads} in the range of 0.1 to 0.4-0.5, depending on R . For larger $\alpha^{ads} (> 0.5)$, the end monomers have the largest charge.

The shape with two minima near the end monomers seems to exist for smaller α^{ads} (≈ 0.2) for all mixing ratios, as evidenced by the location of the minima, $i = 2$ or 3 (Figure S4a). With increased ionization, the charge tends to increase more at the end of the chains. This gives rise to the charge profile with a single minimum near the middle of the adsorbed PE for larger α and the smaller values of R . For $R = 2.0$, the profile with two minima persist even though the charge profile is flatter for larger α , and the global maximum changes from the middle to the ends of the chain. The difference between the maximum and minimum average charge within a chain is, however, not very large (Figure S4c).

Figure S6a shows the radial distribution function for polyacids and counterions. The dashed line refers to a fully ionized polyacid in the absence of the NP. For $R = 1.0$, the NP is nearly neutralized by the polyacids and the number of polyacid-associated counterion is significantly lower. As the total polyacid charge in the system is increased, by increasing α or R , the counterion are increasingly attracted to the polyacid. The bump close to 50 \AA corresponds to the diameter of the NP with a monolayer of polyacid on both sides (48 \AA), that is, it corresponds to adsorption of counterions on the polyacid chains on the opposite side of the NP. From inspecting snapshots of the systems, we observe more counterions close

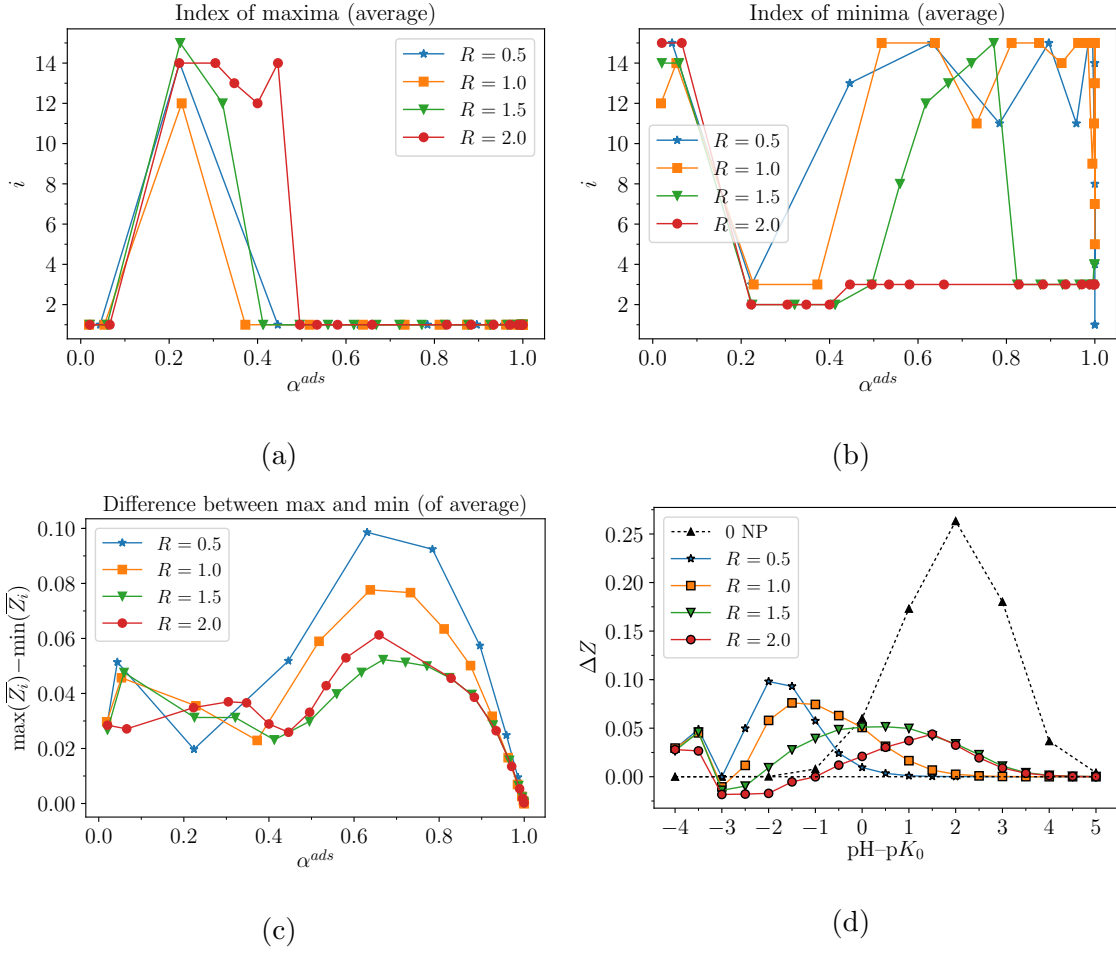


Figure S4: (a)-(b) Index of $\max(\bar{Z}_i)$ and $\min(\bar{Z}_i)$, respectively, as a function of α^{ads} . (c) Charge difference between the maxima and minima. (d) Same as Figure 4, but as function of $\text{pH} - \text{p}K_0$.

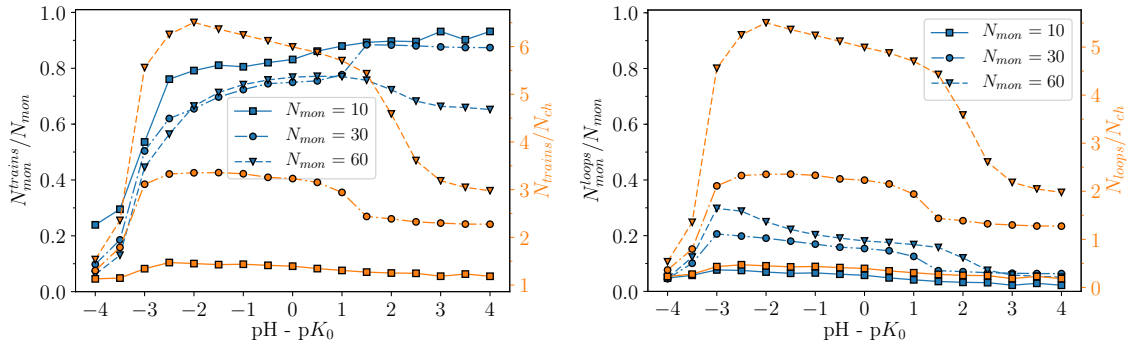
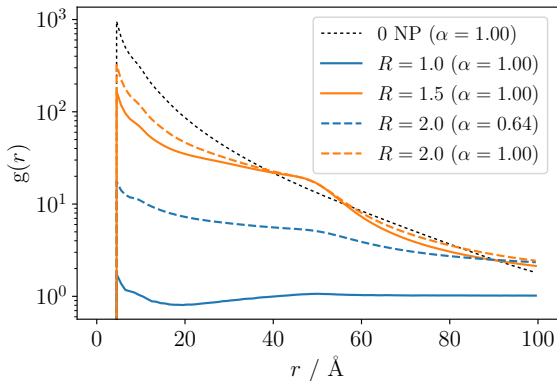
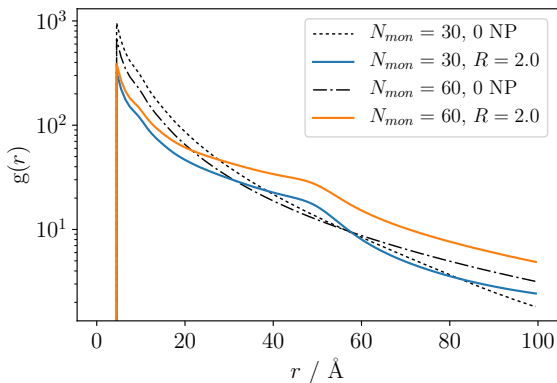


Figure S5: Train and loop characteristics for the same systems as in Figure 6a.

to the free chain than to the polyacid-NP complex in the case of $N_{mon} = 30$. For $N_{mon} = 60$, it is observed that the counterion density is higher in the vicinity of the tail when compared to the central part of the complex.



(a)



(b)

Figure S6: Radial distribution functions for (a) polyacid and positive counterion with $N_{mon} = 30$ and (b) for polyacid and positive counterion for fully charged chains ($\alpha = 1$).

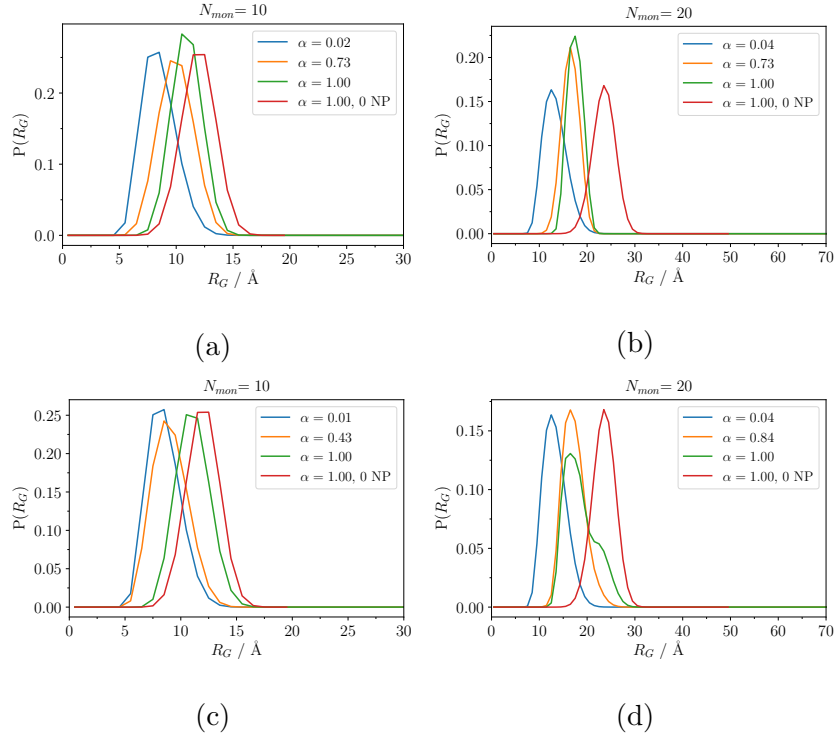


Figure S7: Probability distribution of the gyration radius R_G at different degrees of ionization. (a)-(b) display results for systems with mixing ratio $R = 1$ at $N_{mon} = 10$ and 20, respectively. (c)-(d) show results for $R = 2$. As can be seen, all the distributions are unimodal, but at $N_{mon} = 20, R = 2$, there is a small bump for $\alpha = 1$ due to the extended free chains.